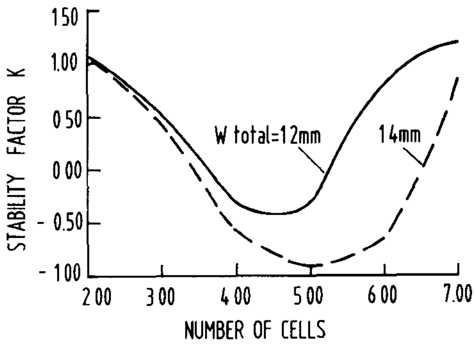

Fig. 6 Effect of the number of cells on amplifiers with the same total gate width.

that the amplifier can be unstable at $F_c = 19$ GHz and when g_{m0} becomes greater than 200 mS/mm (Fig. 5).

If the transconductance g_m changes from 145 mS/mm to 200 mS/mm, the theoretical gain curve in Fig. 5 presents a very high gain around 20 GHz. The stability coefficient K becomes less than unity in this frequency range and the amplifier oscillates at 20.5 GHz. The small difference between this value and the predicted oscillation frequency (F_0) is due to the simplified model used for the analysis.

To improve the gain, another possibility for distributed amplifier design is to increase the number of cells. To improve the frequency bandwidth or the flatness of the gain, the same technique can be used but with smaller transistors.

It is of interest to compare amplifiers with the same total gate width but with a different number of cells.

Fig. 6 presents the minimum stability coefficient K of different amplifiers based on the FET equivalent circuit in Section III (Table II) with $g_{m0} = 250$ mS/mm and at frequency f_0 (eq. (6)). Two total gate widths have been considered. It can be seen that to avoid instability, smaller total gate widths have to be used. However, the lowest value is limited by the decreasing gain–bandwidth product. Fig. 7 also shows that instabilities occur with an increase in the number of cells. This phenomenon is caused by the multiple feedback loops in the amplifier. However, it is considerably diminished when the losses are increased where a large number of cells are used.

IV. Distributed Amplifier with Cascode Pairs

It is well known that using cascode pairs increases the gain of distributed amplifiers. Moreover, the better isolation of this arrangement should attenuate the oscillation phenomenon when the transconductance is increased. This means that the reduction of the coupling between the gate and drain lines makes it possible to avoid oscillations by reducing the gain within the loop.

But another problem occurs in cascode distributed amplifiers. Indeed, the insertion of transmission line lengths between common-source and common-gate FET's is extensively used to increase the gain at high frequency and also to tune the gain response of the amplifier for optimum gain flatness. But these line lengths can generate oscillations and therefore must be carefully chosen as a function of the transconductance of the active devices.

V. Conclusion

The occurrence of oscillations in distributed amplifiers has been evaluated. The oscillation mechanism has been elucidated using a simplified transistor model made up of four elements.

The analysis has been extended to amplifiers whose transistors are represented by S-parameter derived models. It has been demonstrated that increasing the transconductance of the transistor can generate oscillations into the loops existing in distributed amplifiers between stages at frequencies around

$$f_0 \frac{1}{\pi * \sqrt{2L(C + C_{gd})}}.$$

This phenomenon occurs when high-transconductance transistors are used (HEMT devices, for example) and it can be reduced using smaller transistors or higher cutoff frequencies.

Improvements in the gain–bandwidth product can be obtained with high transconductances but need lower gate-to-drain feedback capacitances or other structures such as the cascode configuration to reduce the coupling effect between the gate and drain lines.

Acknowledgment

The author wishes to thank Y. Deville and V. Pauker for helpful discussions.

References

[1] R. Pauley, P. Asher, J. M. Schellenberg, and H. Yamasaki, "A 2 to 40 GHz monolithic distributed amplifier," presented at GaAs IC Symp., Nov. 1985.
[2] J. Orr, "A stable 2–26.5 GHz two stages dual-gate distributed MMIC amplifier," presented at IEEE Monolithic Circuit Symp., June 1986.
[3] K. B. Niclas, W. T. Wilser, R. T. Kritzer, and R R. Pereira, "On theory and performance of solid-state microwave distributed amplifiers," *IEEE Trans. Microwave Theory Tech* , vol. MTT-31, pp. 447–456, June 1983.
[4] P. Gamand, "A complete small size 2 to 30 GHz hybrid distributed amplifier using a novel design technique," in *IEEE MTT Symp. Dig.*, June 1986.
[5] J. B. Beyer, S. N. Prasad, R. C. Becker, J. E. Nordman, and G. K. Hohenwarter, "MESFET distributed amplifier design guidelines," *IEEE Trans. Microwave Theory Tech.*, vol. MTT-32, Mar. 1984.
[6] P. Gamand, M. Fairburn, C. Varin, and J. C Meunier, "1 to 20 GHz monolithic distributed amplifier using GaAs MESFET's or HEMT's," presented at 17th European Microwave Conf., Roma, Italy, Sept. 1987.

Lower Bound on the Eigenvalues of the Characteristic Equation for an Arbitrary Multilayered Gyromagnetic Structure with Perpendicular Magnetization

MICHAŁ MROZOWSKI AND JERZY MAZUR

***Abstract* —A layered gyromagnetic waveguiding structure magnetized perpendicularly to interfaces between layers is analyzed. The lower bound on the eigenvalues of the wave equation for this structure is derived using**

Manuscript received December 29, 1987; revised June 15, 1988. This work was supported by the Polish Academy of Sciences under Contract CPBP-02.02-VII-3.2.
The authors are with the Telecommunication Institute, Technical University of Gdańsk, 80-952 Gdańsk, Poland.
IEEE Log Number 8824245.

the spectral theory of linear operators. The elements of the transfer matrix for a layer of a gyromagnetic medium are given. A numerical example confirming the validity of the theoretical results is included.

I. Introduction

Although layered guides containing gyrotropic material are extensively utilized in microwave application [1]–[3], the underlying theory is less developed than the state of the art in the analysis of isotropic structures. For this reason a new, general approach to the analysis of an arbitrary lossless parallel-plate line with inhomogeneous gyromagnetic filling was proposed by the authors [4]. The present paper develops and complements this analysis, yielding exact expressions defining the global lower bound on the eigenvalues of the characteristic equation for a parallel-plate line containing perpendicularly magnetized layers of gyromagnetic media. Such information allows one to limit the region in which the eigenvalues are sought and, as a consequence, to reduce the amount of time needed to carry out numerical computations.

The approximate value of the lower bound could be also obtained via variational calculus [6], [7]. However, the result obtained using this method would depend not only on the physical parameters of the strata but also on the geometry of the structure. In consequence, a change in the dimensions of the line or the location of a layer in the structure would yield a different expression for the lower bound, whereas the formulas derived in this paper are general because they are valid for the whole class of structures.

II. Determination of the Lower Bound on Eigenvalues

In the theoretical study presented in [4] it was shown that the electromagnetic wave propagation in a lossless parallel-plate line filled with perpendicularly magnetized strata of gyromagnetic media (Fig. 1) can be expressed in terms of the following eigenvalue problem:

$$\mathbb{L}\varphi - \delta\varphi = 0 \tag{1a}$$

$$\mathbb{B}(\varphi) = 0. \tag{1b}$$

In the above equations $\mathbb{B}$ represents the boundary conditions at $x = x_0, x = x_N$, $\mathbb{L}$ is a linear differential operator whose elements are given in Appendix I, and δ and φ denote the eigenvalue and vector eigenfunction, respectively.

In order to determine the lower bound on the eigenvalues of operator $\mathbb{L}$ we will use properties of positive definite operators [5], i.e., self-adjoint linear operators for which the inequality

$$\langle \mathbb{A}x, x\rangle > 0$$

is valid for all functions x taken from the domain $(X, \langle\ ,\ \rangle)$. The eigenvalues of a positive definite operator are positive. Operator $\mathbb{L}$ defined by equations (A2) is not positive definite. However, for the inner product defined by

$$\langle \boldsymbol{u}, \boldsymbol{v}\rangle = \int_{x_0}^{x_N} [\epsilon^{-1}(x)u_1(x)v_1(x) + u_2(x)v_2(x)]\,dx \tag{2}$$

where $\boldsymbol{u} = \mathrm{col}[u_1(x), u_2(x)]$ and $\boldsymbol{v} = \mathrm{col}[v_1(x), v_2(x)]$, operator $\mathbb{L}$ is self-adjoint [4].

To find the lower bound on its eigenvalues let us subtract and add to (1a) the term $\delta'\varphi$ where δ' is a real constant. As a result we obtain

$$\mathbb{L}\varphi - \delta'\varphi + \delta'\varphi - \delta\varphi = 0. \tag{3}$$

Let us denote $\bar{\mathbb{L}} = \mathbb{L} - \delta'$ and $\bar{\delta} = \delta - \delta'$. Introducing these symbols into (3) we get the following operator equation:

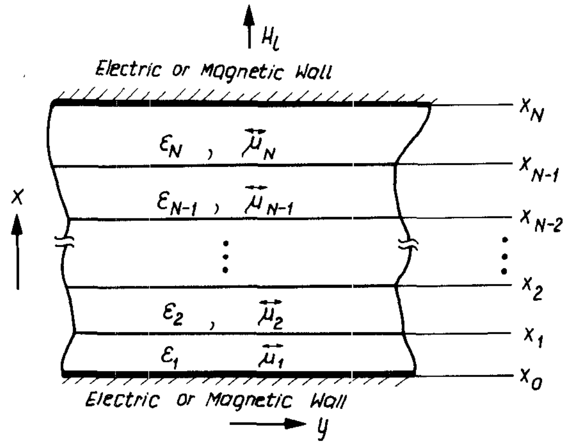

Fig 1. Cross section of a multilayered parallel-plate line filled with gyromagnetic media.

$$\bar{\mathbb{L}}\varphi - \bar{\delta}\varphi = 0. \tag{4}$$

In this way a new eigenvalue problem is defined. Note that $\bar{\mathbb{L}}$ is a self-adjoint operator. Moreover, the eigenvalue problems (1a) and (4) are equivalent because they lead to an identical set of eigenfunctions. There is a simple relation between the eigenvalues δ_i of $\mathbb{L}$ and eigenvalues $\bar{\delta}_i$ of $\bar{\mathbb{L}}$, namely,

$$\delta_i = \bar{\delta}_i + \delta'. \tag{5}$$

Having defined operator $\bar{\mathbb{L}}$ let us test the inequality

$$\langle \bar{\mathbb{L}}\varphi, \varphi\rangle > 0. \tag{6}$$

Using (1) and (A2) together with the definition of the inner product (2) and integrating the resulting expressions by parts, we get

$$\langle \bar{\mathbb{L}}\varphi, \varphi\rangle = \int_{x_0}^{x_N}\left\{\frac{1}{\epsilon(x)}(\nabla_x\varphi_1)^2 - k_0^2\mu_{\mathrm{eff}}(x)\varphi_1^2 - \frac{\delta'}{\epsilon(x)}\varphi_1^2 + 2k_0\frac{\kappa(x)}{\mu(x)}\varphi_1\nabla_x\varphi_2 + \frac{1}{\mu(x)}(\nabla_x\varphi_2)^2 - k_0^2\epsilon(x)\varphi_2^2 - \delta'\varphi_2^2\right\}dx.$$

Now we make the following substitution:

$$2k_0\frac{\kappa(x)}{\mu(x)}\varphi_1\nabla_x\varphi_2 = \frac{1}{\mu(x)}(k_0\kappa(x)\varphi_1 + \nabla_x\varphi_2)^2 - \frac{k_0^2\kappa^2(x)}{\mu(x)}\varphi_1^2 - \frac{1}{\mu(x)}(\nabla_x\varphi_2)^2.$$

Bearing in mind that

$$\mu_{\mathrm{eff}}(x) = \frac{\mu^2(x) - \kappa^2(x)}{\mu(x)}$$

we obtain

$$\langle \bar{\mathbb{L}}\varphi, \varphi\rangle = \int_{x}^{x_N}\left\{\frac{1}{\epsilon(x)}(\nabla_x\varphi_1)^2 + \frac{1}{\mu(x)}[k_0\kappa(x)\varphi_1 + \nabla_x\varphi_2]^2 - \left[k_0^2\mu(x) + \frac{\delta'}{\epsilon(x)}\right]\varphi_1^2 - [k_0^2\epsilon(x) + \delta']\varphi_2^2\right\}dx.$$

In the above equations k_0 is the wavenumber in free space, and $\epsilon(x)$, $\mu(x)$, and $\kappa(x)$ are the relative permittivity and the diagonal and off-diagonal elements of the relative permeability tensor of the gyromagnetic material, respectively. The scalar operator ∇_x is used to represent the partial derivative $\partial/\partial x$.

We can now exclude the case of negative values of μ. It is seen that in the above expression the first two terms are always

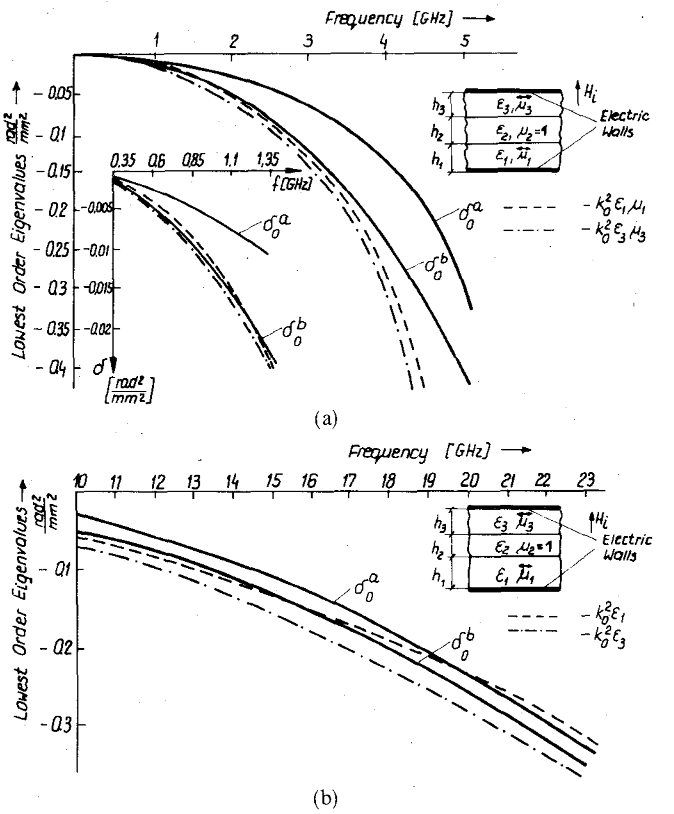

Fig. 2. The lowest order eigenvalues of an asymmetrical ferrite–dielectric–ferrite parallel-plate line (δ_0^a for $h_2=1$ mm, $h_3=3$ mm; δ_0^b for $h_2=0$ mm, $h_3=4$ mm; $M_{s1}=167.11$ kA/m, $M_{s3}=139.26$ kA/m, $H_i=159.24$ kA/m, $\epsilon_1=13.5$, $\beta\epsilon_2=2.6$, $\epsilon_3=16$, $h_1=1.5$ mm). (a) Below the ferromagnetic resonance. (b) Above the ferromagnetic resonance.

positive; therefore the inequality (6) is true if both

$$k_0^2\epsilon(x)\mu(x)+\delta'\leqslant 0$$

and

$$k_0^2\epsilon(x)+\delta'\leqslant 0. \tag{7}$$

Let us denote by M the greater of the numbers $M_1=\max(k_0^2\epsilon_k\mu_k)$ and $M_2=\max(k_0^2\epsilon_k)$, for $k=1,2,\cdots,N$. We may now conclude from (7) that if only M is finite then $\bar{\mathbb{L}}$ is positive definite for every $\delta'\leqslant -M$, and in such a case all its eigenvalues are positive. Because the eigenvalues of one operator are related to the eigenvalues of the other, we get, according to (5), the following expression defining the lower bound on δ_i:

$$\delta_i > -M \tag{8}$$

with $M=\max(k_0^2\epsilon_k\mu_k, k_0^2\epsilon_k)$, $k=1,\cdots,N$.

III. Numerical Verification

In order to verify the results derived in the previous section an exemplary structure of an asymmetrical ferrite–dielectric–ferrite parallel-plate line was investigated. The characteristic equation for the structure was obtained using the normal field components approach described thoroughly in [4]. Detailed expressions for the elements of the transfer matrix for a single gyromagnetic layer are given in Appendix II. A region in which either μ_1 or μ_3 is negative was excluded from numerical computations. The results are shown in Fig. 2. For the investigated line condition (8) can be formulated as

$$\delta_i > -k_0^2\epsilon_3\mu_3 \qquad \text{for } 0<f<\bar{\gamma}H_i$$

and (9)

$$\delta_i > -k_0^2\epsilon_3 \qquad \text{for } f>\bar{\gamma}\left[H_i(H_i+M_{s1})\right]^{1/2}$$

where $\bar{\gamma}$, H_i, M_{sk}, and ϵ_k are the gyromagnetic ratio, the internal biasing magnetic field, the saturation magnetization, and the relative permittivity of the kth layer, respectively. From the diagram it is seen that curves $\delta(f)$ are situated above the lines corresponding to the theoretically obtained limits, and accordingly satisfy conditions (9).

IV. Conclusions

Exact expressions have been derived for the lower bound on the eigenvalues of the characteristic equation for an arbitrary multilayered gyromagnetic structure magnetized perpendicularly to the interfaces between layers. The approach is universal and allows one to determine bounds on the eigenvalues for a wider class of lossless structures filled with inhomogeneous anisotropic medium. The result is general and useful since it enables one to minimize the cost of numerical computations. The theoretical predictions found confirmation in a numerical example.

Appendix I
Definition of the Elements of Operator $\mathbb{L}$

Operator $\mathbb{L}$ has the following matrix representation:

$$\mathbb{L}=\begin{bmatrix}\mathbb{L}_{11} & \mathbb{L}_{12}\\ \mathbb{L}_{21} & \mathbb{L}_{22}\end{bmatrix} \tag{A1}$$

with

$$\mathbb{L}_{11}=-\epsilon(x)\nabla_x\left[\frac{1}{\epsilon(x)}\nabla_x\right]-k_0^2\mu_{\text{eff}}(x)\epsilon(x) \tag{A2a}$$

$$\mathbb{L}_{12}=k_0\epsilon(x)\frac{\kappa(x)}{\mu(x)}\nabla_x \tag{A2b}$$

$$\mathbb{L}_{21}=-\nabla_x\left[k_0\frac{\kappa(x)}{\mu(x)}\right] \tag{A2c}$$

$$\mathbb{L}_{22}=-\nabla_x\left[\frac{1}{\mu(x)}\nabla_x\right]-k_0^2\epsilon(x). \tag{A2d}$$

Appendix II
Transfer Matrix for a Single Layer of a Gyromagnetic Medium

The characteristic equation for an arbitrary multilayered perpendicularly magnetized gyromagnetic structure can be obtained using the method described in [4]. Depending on the combination of boundary conditions at $x=x_0$ and $x=x_N$, the characteristic equation is the determinant of one of the submatrices of the global transfer matrix $\boldsymbol{I}$, where $\boldsymbol{I}$ is defined as

$$\boldsymbol{I}=\prod_{i=1}^{N}\boldsymbol{I}^{(i)}. \tag{A3}$$

$\boldsymbol{I}^{(i)}$ is a transfer matrix linking the continuity vector $\boldsymbol{F}^{(i)}$ between the extremes x_i^- and x_{i-1}^+ of the ith layer:

$$\boldsymbol{F}^{(i)}_{|x=x_i^-}=\boldsymbol{I}^{(i)}\boldsymbol{F}^{(i)}_{|x=x_{i-1}^+} \tag{A4}$$

where

$$\boldsymbol{F}^{(i)}=\begin{bmatrix}\frac{1}{\epsilon_i}\nabla_x & 0 & 1 & \frac{\kappa_i}{\mu_i}k_0\\ 0 & 1 & 0 & \frac{1}{\mu_i}\nabla_x\end{bmatrix}^T\begin{bmatrix}D_x^i\\ \epsilon_0\eta_0H_x^i\end{bmatrix}. \tag{A5}$$

Elements of the transfer matrix $I^{(i)}$ are given by the following expressions:

$$T_{11}^{i}=\frac{1}{M_1}(\lambda_1 S_1 R_3 ch(\lambda_1 h_i)-\lambda_3 ch(\lambda_3 h_i)) \quad \text{(A6)}$$

$$T_{21}^{i}=\epsilon_i\frac{R_3}{M_1}(ch(\lambda_1 h_i)-ch(\lambda_3 h_i)) \quad \text{(A7)}$$

$$T_{31}^{i}=\epsilon_i\frac{1}{M_1}(S_1 R_3 sh(\lambda_1 h_i)-sh(\lambda_3 h_i)) \quad \text{(A8)}$$

$$T_{41}^{i}=\epsilon_i\frac{1}{M_1}(R_3 G_1 sh(\lambda_1 h_i)-G_3 sh(\lambda_3 h_i)) \quad \text{(A9)}$$

$$T_{12}^{i}=\frac{S_1\lambda_1\lambda_3}{M_1\epsilon_i}(-ch(\lambda_1 h_i)+ch(\lambda_3 h_i)) \quad \text{(A10)}$$

$$T_{22}^{i}=\frac{1}{M_1}(-\lambda_3 ch(\lambda_1 h_i)+R_3 S_1\lambda_1 ch(\lambda_3 h_i)) \quad \text{(A11)}$$

$$T_{32}^{i}=\frac{S_1}{M_1}(-\lambda_3 sh(\lambda_1 h_i)+\lambda_1 sh(\lambda_3 h_i)) \quad \text{(A12)}$$

$$T_{42}^{i}=\frac{1}{M_1}(-\lambda_3 G_1 sh(\lambda_1 h_i)+G_3 S_1\lambda_1 sh(\lambda_3 h_i)) \quad \text{(A13)}$$

$$T_{13}^{i}=\frac{1}{M_2\epsilon_i}(\lambda_1 S_1 G_3 sh(\lambda_1 h_i)-\lambda_3 G_1 sh(\lambda_3 h_i)) \quad \text{(A14)}$$

$$T_{23}^{i}=\frac{1}{M_2}(G_3 sh(\lambda_1 h_i)-G_1 R_3 sh(\lambda_3 h_i)) \quad \text{(A15)}$$

$$T_{33}^{i}=\frac{1}{M_2}(S_1 G_3 ch(\lambda_1 h_i)-G_1 ch(\lambda_3 h_i)) \quad \text{(A16)}$$

$$T_{43}^{i}=\frac{G_1 G_3}{M_2}(ch(\lambda_1 h_i)-ch(\lambda_3 h_i)) \quad \text{(A17)}$$

$$T_{14}^{i}=\frac{S_1}{M_2\epsilon_i}(-\lambda_1 sh(\lambda_1 h_i)+\lambda_3 ch(\lambda_3 h_i)) \quad \text{(A18)}$$

$$T_{24}^{i}=\frac{1}{M_2}(-sh(\lambda_1 h_i)+R_3 S_1 sh(\lambda_3 h_i)) \quad \text{(A19)}$$

$$T_{34}^{i}=\frac{S_1}{M_2}(-ch(\lambda_1 h_i)+ch(\lambda_3 h_i)) \quad \text{(A20)}$$

$$T_{44}^{i}=\frac{1}{M_2}(-G_1 ch(\lambda_1 h_i)+G_3 S_1 ch(\lambda_3 h_i)) \quad \text{(A21)}$$

where

$$M_1=R_3 S_1\lambda_1-\lambda_3 \qquad M_2=S_1 G_3-G_1$$
$$G_1=\frac{\kappa_i k_0 S_1+\lambda_1}{\mu_i} \qquad G_3=\frac{\kappa_i k_0+R_3\lambda_3}{\mu_i} \quad \text{(A22)}$$
$$h_i=x_i-x_{i-1}$$

whereas

$$S_1=-\frac{1}{k_0\kappa_i\lambda_1}\left[\lambda_1^2+\mu_i(\delta+k_0^2\epsilon_i)\right] \quad \text{(A23)}$$

$$R_3=\frac{\mu_i}{k_0\kappa_i\epsilon_i\lambda_3}\left(\lambda_3^2+\delta+k_0^2\epsilon_i\mu_{\text{eff}_i}\right) \quad \text{(A24)}$$

$$\lambda_{1(3)}=\left\{\frac{1}{2}\left[g_2\mp\left(g_2^2-4g_0\right)^{1/2}\right]\right\}^{1/2} \quad \text{(A25)}$$

with

$$g_2=-\delta(1+\mu_i)-2k_0^2\epsilon_i\mu_i \quad \text{(A26)}$$

$$g_0=\mu_i\left(\delta+k_0^2\epsilon_i\mu_{\text{eff}_i}\right)\left(\delta+k_0^2\epsilon_i\right). \quad \text{(A27)}$$

ACKNOWLEDGMENT

The authors wish to thank L. Hayes for her assistance during preparation of this paper.

REFERENCES

[1] I. Awai and T. Itoh, "Multilayered open dielectric waveguide with a gyrotropic layer," *Int. J. Infrared and Millimeter Waves*, vol. 2, no. 1, pp 1–14, 1981.
[2] I. Awai and T Itoh, "Coupled-modes theory analysis of distributed nonreciprocal structures," *IEEE Trans. Microwave Theory Tech.*, vol. MTT-29, pp. 1077–1087, Oct 1981.
[3] A. Beyer, "Ferrite devices in finline technique for integrated millimeter-wave circuits," in *Proc. 8th. Colloq. Microwave Communication* (Budapest) 1986, pp. 219–220.
[4] M. Mrozowski and J. Mazur, "General analysis of a parallel-plate waveguide inhomogeneously filled with gyromagnetic media," *IEEE Trans. Microwave Theory Tech.*, vol MTT-34, pp. 388–395, Apr. 1986.
[5] A. Wouk, *A Course of Applied Functional Analysis.* New York: Wiley, 1979.
[6] P. M. Morse and H. Feshbach, *Methods of Theoretical Physics.* New York, McGraw-Hill, 1953
[7] A. D. Berk, "Variational principles for electromagnetic resonators and waveguides," *IRE Trans. Antennas Propagat.*, pp. 104–111, Apr. 1956

Effects of Gain Compression, Bias Conditions, and Temperature on the Flicker Phase Noise of an 8.5 GHz GaAs MESFET Amplifier

C. P. LUSHER AND W. N. HARDY

***Abstract*—We have measured the phase noise of an 8.5 GHz GaAs MESFET amplifier at temperatures from 1.7 K to 300 K for input powers from −30 dBm to well past the 1 dB gain compression point and for sideband frequencies from 0.1 Hz to 25 kHz. The observed flicker phase noise was independent of input power, even at levels producing 4 dB of gain compression, and also changed very little with bias conditions. The intrinsic phase noise at low temperatures (observed below 2.17 K, where an extrinsic effect due to the bubbling of the liquid helium coolant disappears) was slightly higher than that observed at room temperature. However, we saw no sign of the dramatic increase in flicker phase noise at low**

Manuscript received April 6, 1988; revised October 5, 1988. This work was supported by the National Research Council of Canada and by the Natural Sciences and Engineering Research Council of Canada.
C. P. Lusher was with the Department of Physics, University of British Columbia, Vancouver, B.C., Canada V6T 2A6. He is now with the Department of Physics, Royal Holloway and Bedford New College, University of London, Egham Hill, Egham, Surrey, TW20 0EX, England.
W. N. Hardy is with the Department of Physics, University of British Columbia, Vancouver, B.C., Canada V6T 2A6.
IEEE Log Number 8825394.